CHEMISTRY
AN ASIAN JOURNAL

DOI: 10.1002/asia.200600404

Alcohol-Vapor Inclusion in Single-Crystal Adsorbents $[M^{II}_2(bza)_4(pyz)]_n$ (M = Rh, Cu): Structural Study and Application to Separation Membranes

Satoshi Takamizawa,*[a] Chihiro Kachi-Terajima,[a] Masa-aki Kohbara,[a] Takamasa Akatsuka,[a] and Tetsuro Jin*[b]

Abstract: The vapor absorbency of the series of alcohols methanol, ethanol, 1-propanol, 1-butanol, and 1-pentanol was characterized on the single-crystal adsorbents $[M^{II}_2(bza)_4(pyz)]_n$ (bza = benzoate, pyz = pyrazine, M = Rh (**1**), Cu (**2**)). The crystal structures of all the alcohol inclusions were determined by single-crystal X-ray crystallography at 90 K. The crystal-phase transition induced by guest adsorption occurred in the inclusion crystals except for 1-propanol. A hydrogen-bonded dimer of adsorbed alcohol was found in the methanol- and ethanol-inclusion crystals, which is similar to a previous observation in **2**·2EtOH (S. Takamizawa, T. Saito, T. Akatsuka, E. Nakata, *Inorg. Chem.* **2005**, *44*, 1421–1424). In contrast, an isolated monomer was present in the channel for 1-propanol, 1-butanol, and 1-pentanol inclusions. All adsorbed alcohols were stabilized by hydrophilic and/or hydrophobic interactions between host and guest. From the combined results of microscopic determination (crystal structure) and macroscopic observation (gas-adsorption property), the observed transition induced by gas adsorption is explained by stepwise inclusion into the individual cavities, which is called the "step-loading effect." Alcohol/water separation was attempted by a pervaporation technique with microcrystals of **2** dispersed in a poly(dimethylsiloxane) membrane. In the alcohol/water separation, the membrane showed effective separation ability and gave separation factors (alcohol/water) of 5.6 and 4.7 for methanol and ethanol at room temperature, respectively.

Keywords: adsorption · alcohols · crystal structures · host–guest systems · pervaporation

Introduction

Porous materials based on metal–organic compounds are attractive research targets owing to their designable structure, unusual flexibility, and tunable functional groups.[1] Control of the inclusion phenomenon is one of the most important issues for applications of molecular recognition and separation. The channel structures can be designed and modified by tuning the host properties, for example, cavity size, shape, and intermolecular interactions for the included guests, such as π–π, dipole–dipole, and hydrophobic interactions. Guest reactivity and stability can also be controlled in the cavity.[2] The remarkable feature of these materials is their reversible structural transformation in the adsorption process.[1,3] Such a flexible host lattice that adapts to the characteristics of the guest would contribute to progress in molecular-recognition techniques. Direct crystallographic observation of inclusion crystals through gas (or vapor) adsorption would reveal clearly the physicochemical properties of the adsorbed guests.[4] Recently, we synthesized the single-crystal adsorbents $[M^{II}_2(bza)_4(pyz)]_n$ (bza = benzoate, pyz = pyrazine, M = Rh (**1**), Cu (**2**)) (Scheme 1).[5,6] These complexes have a 1D chain skeleton, which is the same as the previous example of a Cu^{II} benzoate–pyrazine complex[7] except that they crystallize in a different packing mode. Because their single crystals retain their crystallinity and shape after guest adsorption, an opportunity to determine the exact aggregate structure of various accommodated guests by conventional single-crystal X-ray diffraction analysis is presented.[8,9] In our previous study, we revealed the exten-

[a] Dr. S. Takamizawa, Dr. C. Kachi-Terajima, M.-a. Kohbara, T. Akatsuka
International Graduate School of Arts and Sciences
Yokohama City University
22-2 Seto, Kanazawa-ku, Yokohama 236-0027 (Japan)
Fax: (+81)45-787-2187
E-mail: staka@yokohama-cu.ac.jp

[b] Dr. T. Jin
National Institute of Advanced Industrial Science & Technology (AIST)
1-8-31 Midorigaoka, Ikeda, Osaka 563-8577 (Japan)
Fax: (+81)727-51-9627
E-mail: tetsu-jin@aist.go.jp

Supporting information for this article is available on the WWW under http://www.chemasianj.org or from the author.

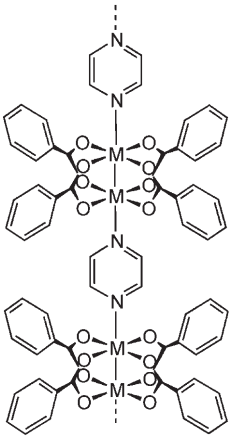

Scheme 1. Infinite chain structure of $[M^{II}_2(bza)_4(pyz)]_n$ (**1**: M = Rh; **2**: M = Cu).

sive gas-adsorption ability of these complexes with both inorganic and organic guests. Alcohol molecules may be good candidates for investigating the aggregate state within a channel because of the low-symmetry structure with both hydrophilic and hydrophobic groups. Recently, alcohol recognition and its inclusions were studied primarily in intercalation by using layered or interpenetrated host structures.[10] Although several examples of the structural determination of adsorbed alcohols by soaking in liquid have been reported based on single-crystal X-ray diffraction analysis,[11] studies based on alcohol-vapor adsorption into empty crystals are rare.[4d] We reported the successful determination of the ethanol-inclusion structure **2**·2EtOH and revealed the occurrence of a phase transition from monoclinic *C*2/*c* to triclinic $P\bar{1}$ induced by alcohol-vapor adsorption. In this ethanol inclusion, the hydrogen-bonded dimer was generated in the channel, which cocrystallized with the host lattice.[9] To prove the ability of adsorbents **1** and **2** to adjust to diverse guest characteristics such as size, shape, and alkyl-chain length, we prepared the following alcohol-inclusion crystals systematically through the vapor-adsorption process: methanol, ethanol, 1-propanol, 1-butanol, and 1-pentanol. Herein, we report the alcohol-adsorption properties and the exact aggregate structure of alcohols in **1** and **2** and discuss them in relation to the hydrophilic and hydrophobic interactions between the guest and the channel wall (Figure 1).

	Methanol	Ethanol	1-Propanol	1-Butanol	1-Pentanol
M_r	32.04	46.07	60.10	74.12	88.15
P_0 [mmHg] at 20°C	97.30	44.06	14.56	4.42	1.43

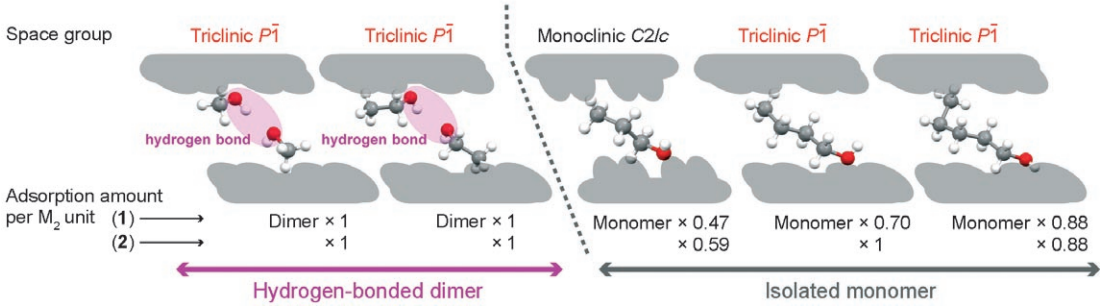

Figure 1. Schematic representation of the aggregation structures of the alcohols, which depend on their molecular properties. Table: Molecular weights and saturated vapor pressures.

Abstract in Japanese:

ガス吸着によって結晶構造を変化させる単結晶ホスト $[M^{II}_2(bza)_4(pyz)]_n$ (M = Rh, Cu) を用いて、アルコール蒸気吸着挙動ならびにホスト結晶構造変化／ゲスト会合構造に与えるアルコール（メタノールからペンタノール）鎖長の影響について調べた。単結晶 X 線構造解析より、鎖の伸長によって水素結合二量体から孤立分子へと安定なゲスト状態の遷移が見られた。また、プロパノール以外の包接結晶では全て吸着誘起の結晶相転移が観測された。これらの結果は吸着測定の結果とも良い一致を示した。また、分離膜技術への応用として、PDMS 分散膜を用いてアルコール／水混合物の膜分離機能について検討し、アルコールの選択分離濃縮特性を明らかにした。

Metal–organic porous crystals and molecular crystals are useful for selective sorption of specific guests because of the flexibility, integrity, and regularity of their pores.[3a,12] This selectivity can be applied to gas storage and separation. However, only a few examples based on such materials are known: selective hydrogen adsorption from CO_2/H_2 mixtures[13] and selective gas-chromatographic separation of alkane mixtures.[14] Because our single-crystal system has a hydrophobic surface,[5] its application to alcohol/water separation is potentially likely. The considerable structural flexibility found in this system would offer novel selectivity of guest molecules compared with conventional adsorbents. Alcohol/water separation is particularly necessary for alcohols produced by biomass conversion because this fuel must be highly concentrated. Pervaporation is well-known to be a

promising membrane-separation technique for water/organic separation, in which a fraction of the liquid is selectively vaporized through the membrane.[15] A great deal of effort has been devoted to the preparation of membranes that incorporate the porous materials of zeolite.[16] In this paper, we report an application to alcohol/water separation by pervaporation by using a mixed-matrix membrane that consists of the single-crystal channel solid **2** dispersed in poly(dimethylsiloxane) (PDMS), which is the first attempt based on a metal complex.

Results and Discussion

Structural Description

Alcohol-inclusion crystals of methanol, ethanol, 1-propanol, 1-butanol, and 1-pentanol for **1** and **2** were structurally characterized by single-crystal X-ray diffraction analysis at 90 K after exposure to the saturated vapor of the respective alcohol at room temperature (Tables 1 and 2). ORTEP diagrams for all alcohol-inclusion crystals are shown in Figure S1 for **1** and Figure S2 for **2** in the Supporting Information. The in-

Table 1. Crystallographic data for single-crystal host **1** under various conditions.

	1·2CH_3OH	**1**·2C_2H_5OH	**1**·0.47*n*-C_3H_7OH	**1**·0.7*n*-C_4H_9OH	**1**·0.88*n*-$C_5H_{11}OH$
Atmospheric vapor	methanol	ethanol	1-propanol	1-butanol	1-pentanol
Empirical formula	$C_{34}H_{32}N_2O_{10}Rh_2$	$C_{36}H_{36}N_2O_{10}Rh_2$	$C_{33.40}H_{27.74}N_2O_{8.47}$ Rh_2	$C_{34.81}H_{31.02}N_2O_{8.70}Rh_2$	$C_{36.40}H_{34.57}N_2O_{8.88}Rh_2$
Crystal size [mm^3]	0.18×0.16×0.08	0.21×0.18×0.02	0.26×0.14×0.04	0.40×0.14×0.02	0.30×0.22×0.08
M_r [$g\,mol^{-1}$]	834.44	862.49	798.45	822.38	847.93
Crystal system	triclinic	triclinic	monoclinic	triclinic	triclinic
Space group	$P\bar{1}$	$P\bar{1}$	$C2/c$	$P\bar{1}$	$P\bar{1}$
T [K]	90	90	90	90	90
a [Å]	9.5989(11)	9.5854(14)	17.837(2)	9.663(10)	9.699(6)
b [Å]	10.0652(12)	10.4057(15)	9.5841(12)	10.216(10)	10.286(6)
c [Å]	10.8247(17)	10.7987(16)	19.574(2)	11.066(12)	11.163(7)
α [°]	70.423(2)	71.452(3)	90	69.37(2)	68.681(13)
β [°]	65.957(2)	64.982(3)	99.048(2)	66.023(16)	66.009(11)
γ [°]	62.594(2)	63.743(3)	90	63.08(2)	63.503(11)
V [$Å^3$]	833.74(17)	863.9(2)	3304.6(6)	870.7(15)	887.7(9)
Z	1	1	4	1	1
D_{calcd} [$g\,cm^{-3}$]	1.662	1.658	1.605	1.568	1.586
$\mu(Mo_{K\alpha})$ [mm^{-1}]	1.050	1.016	1.053	1.002	0.985
Reflections collected	6139	6482	12020	4303	4736
Independent reflections (R_{int})	4091 (0.0300)	4240 (0.0298)	4129 (0.0565)	3025 (0.0973)	3088 (0.0577)
Goodness of fit	1.099	1.174	1.059	0.989	0.976
$R1$ ($I>2\sigma$ (all data))	0.0492 (0.0676)	0.0588 (0.0695)	0.0672 (0.1072)	0.1005 (0.1867)	0.0937 (0.1411)
$wR2$ ($I>2\sigma$ (all data))	0.1156 (0.1330)	0.1554 (0.1658)	0.1691 (0.1979)	0.2212 (0.2688)	0.2272 (0.2629)
Least diff. peak (hole) [$eÅ^3$]	1.495 (2.080)	2.279 (1.151)	2.313 (1.978)	2.582 (2.121)	1.955 (−2.101)

Table 2. Crystallographic data for single-crystal host **2** under various conditions.

	2·2CH_3OH	**2**·2C_2H_5OH[9]	**2**·0.59*n*-C_3H_7OH	**2**·*n*-C_4H_9OH	**2**·0.88*n*-$C_5H_{11}OH$
Atmospheric vapor	methanol	ethanol	1-propanol	1-butanol	1-pentanol
Empirical formula	$C_{34}H_{32}N_2O_{10}Cu_2$	$C_{36}H_{36}N_2O_{10}Cu_2$	$C_{33.76}H_{28.69}N_2O_{8.59}Cu_2$	$C_{36}H_{34}N_2$ O_9Cu_2	$C_{36.40}H_{34.57}N_2O_{8.88}Cu_2$
Crystal size [mm^3]	0.25×0.20×0.03	0.62×0.20×0.10	0.60×0.15×0.08	0.35×0.20×0.06	0.38×0.18×0.06
M_r [$g\,mol^{-1}$]	755.72	783.77	726.90	765.75	769.21
Crystal system	triclinic	triclinic	monoclinic	triclinic	triclinic
Space group	$P\bar{1}$	$P\bar{1}$	$C2/c$	$P\bar{1}$	$P\bar{1}$
T [K]	90	90	90	90	90
a [Å]	9.7003(8)	9.6813(12)	17.909(5)	9.699(3)	9.692(9)
b [Å]	10.0093(9)	10.3897(13)	9.671(2)	9.981(3)	10.116(10)
c [Å]	10.7582(10)	10.7623(14)	19.197(5)	10.908(3)	10.957(10)
α [°]	70.432(2)	71.088(3)	90	69.085(7)	68.326(16)
β [°]	65.339(2)	64.816(2)	98.270(6)	66.425(6)	65.453(16)
γ [°]	62.375(2)	63.731(2)	90	63.868(5)	63.096(16)
V [$Å^3$]	827.98(13)	866.08(19)	3290.3(14)	847.7(4)	849.4(14)
Z	1	1	4	1	1
D_{calcd} [$g\,cm^{-3}$]	1.516	1.503	1.467	1.500	1.504
$\mu(Mo_{K\alpha})$ [mm^{-1}]	1.345	1.289	1.348	1.313	1.310
Reflections collected	6223	6269	10730	5262	4519
Independent reflections (R_{int})	4201 (0.0212)	3771 (0.0457)	3445 (0.0710)	2973 (0.1086)	
Goodness of fit	1.259	1.341	1.078	0.949	1.064
$R1$ ($I>2\sigma$ (all data))	0.0606 (0.0650)	0.0690 (0.0735)	0.0687 (0.1019)	0.0797 (0.1390)	0.1365 (0.2208)
$wR2$ ($I>2\sigma$ (all data))	0.1659 (0.1766)	0.1835 (0.1855)	0.1709 (0.1946)	0.1722 (0.1991)	0.3383 (0.3870)
Least diff. peak (hole) [$eÅ^3$]	0.828 (−0.954)	1.833 (−0.954)	1.679 (−1.688)	1.101 (−1.055)	1.906 (−2.013)

clusion crystals of **1** and **2** are isostructural, with a similar number of inclusion-guest molecules and the same space group. The compositions determined were **1**·2MeOH, **1**·2EtOH, **1**·0.47(1-PrOH), **1**·0.7(1-BuOH), **1**·0.88(1-PeOH), **2**·2MeOH, **2**·2EtOH,[9] **2**·0.59(1-PrOH), **2**·1-BuOH, and **2**·0.88(1-PeOH), which demonstrate the ability of diffusion and incorporation for all the alcohols. The occupancy factors of the adsorbed alcohol were obtained by refining the *R* factor. One cavity in these adsorbents can accommodate up to two ethanol molecules or up to one alcohol molecule larger than ethanol (1-PrOH, 1-BuOH, and 1-PeOH). Single-crystal adsorbents **1** and **2** showed the high flexibility required to adsorb large alcohols comparable to the diameter of the narrow channel. This channel can concentrate guests from diluted gas under low vapor pressures (P_0 = 14.56 mmHg for 1-propanol, 4.42 mmHg for 1-butanol, and 1.43 mmHg for 1-pentanol at 293 K) and can diffuse and stabilize them by its wall. Except for 1-propanol, all inclusion crystals exhibited the crystal-phase transition induced by the adsorption phenomenon from the α (monoclinic) to the β (triclinic) lattice, as was observed in related adsorbents reported previously.[8] The 1-propanol-inclusion crystals expanded slightly from the empty crystals (*C*2/*c*) by 1.8% for **1** and 1.1% for **2**, which would be related to the absence of phase transitions due to the small amount of adsorption.[17,18] In contrast, through phase transition, the cell volume expanded remarkably by 2.8 and 1.8% for methanol, 6.5 and 6.4% for ethanol, 7.4 and 4.2% for 1-butanol, and 9.5 and 4.4% for 1-pentanol for **1** and **2**, respectively. Interestingly, the cell volume expands with increasing alcohol size; this was clearly observed in **1**. Although the methanol and ethanol molecules occupied about twice the volume of the single molecule through the formation of the hydrogen-bonded dimer in the channel, a considerable change in cell volume was not observed. Therefore, the flexible channels and the softly hydrogen bonded guests cooperatively adapt to each of the structures to form a compact state of inclusion crystals, which can stabilize the cocrystallized state. In the 1-butanol- and 1-pentanol-inclusion crystals of **2**, the cell volume did not increase with the size of the alcohol, thus indicating that its host lattice does not easily transform through the adsorption process. This result is consistent with the observation that a higher relative pressure and greater adsorption amount were required for **2** than for **1** at the beginning of the crystal-phase transition in the adsorption measurements (see below). A slight difference in the torsion angle of the benzoate bridge, (M–M)···($O_{benzoate}$···$O_{benzoate}$), was found between the crystal structures of **1** and **2**. This difference in coordination mode may influence guest diffusion in the channel and result in the above-mentioned differences in adsorption behavior and volume change. However, in crystallography, the reason remains unclear.

Hydrogen-Bonded Pairing of Methanol and Ethanol

Tail (OH)-to-tail hydrogen-bonded pairing of guest molecules was found in the methanol- and ethanol-inclusion crystals. These dimers showed centrosymmetric disorder, as was already reported in the ethanol-inclusion crystal of **2**.[9] Hydrophilic interactions between guest and host were also found in the methanol- and ethanol-inclusion crystals through the OH moiety of alcohol and the carboxylate oxygen atoms of the host lattice. The packing views are shown in Figure 2 for **1** and Figure 3 for **2**. The surface views (Figure 4 for **1** and Figure 5 for **2**) illustrate the guest–guest contacts. The short contacts between host and guest are depicted in Figure 6 for **1** and Figure 7 for **2**. Selected guest–guest and host–guest contacts are listed in Table 3. The methanol- and ethanol-inclusion crystals exhibited the same hydrogen-bonded core, O–H(guest)···O–H(guest)···O(host), with strong guest–guest interactions (O···O = 2.793(18) Å for **1**·2MeOH, 2.800(17) Å for **2**·2MeOH, 2.75(2) Å for **1**·2EtOH, and 2.75(1) Å for **2**·2EtOH),[9] and weak host–guest interactions (O···O = 3.293(8) Å for **1**·2MeOH, 3.017(8) Å for **2**·2MeOH, 3.569(10) Å for **1**·2EtOH, and 3.031(8) Å for **2**·2EtOH).[9] The hydrophobic interactions between the alkyl chain of the alcohol and the surrounding benzoate and pyrazine rings were more effective in ethanol inclusion than in methanol inclusion. Although the hydrogen bond in the methanol dimer is expected to be stronger than that in the ethanol dimer, the methanol dimer is less stable in the channel than the included ethanol dimer because of its smaller surface area. However, selective generation of the hydrogen-bonded dimer was found for methanol, which indicates that these hosts can stabilize guests by a structural change of their flexible channels.

Isolated State of 1-Propanol, 1-Butanol, and 1-Pentanol

The longer alcohols 1-propanol, 1-butanol, and 1-pentanol were isolated in each channel of crystals **1** and **2**. The surface views are shown in Figure 4 for **1** (Figure 5 for **2**). The host–guest short contacts are depicted in Figure 6 for **1** and Figure 7 for **2**, and their relevant bond distances are summarized in Table 4. The isolated guest molecules were observed in unique positions in the channel; they bear a centrosymmetric disorder that corresponds to the host-crystal symmetry. Interestingly, the expected positional disorder and multiple conformations were not observed in the crystal structure. The included alcohol molecules were separated from the nearest molecules along the channel by a minimum guest–guest distance of C···C = 6.24(5) Å for 1-propanol, 6.01(14) Å for 1-butanol, and 5.69(5) Å for 1-pentanol in **1**, and C···C = 6.15(3) Å for 1-propanol, C···C = 6.26(4) Å for 1-butanol, and O···O = 5.44(4) Å for 1-pentanol in **2**. The included 1-propanol molecule formed a weak hydrogen bond to the benzoate oxygen of the host with O···O distances of 3.19(3) Å for **1** and 3.327(19) Å for **2**. The O–H···π interaction was only observed in **2** for the 1-butanol-inclusion crystal with an O···C distance of 3.239(14) Å. In the 1-butanol- and 1-pentanol-inclusion crystals, no hydrogen bond was found either between host and guest or between guests. The alkyl moiety of all the alcohol molecules contacts the hydro-

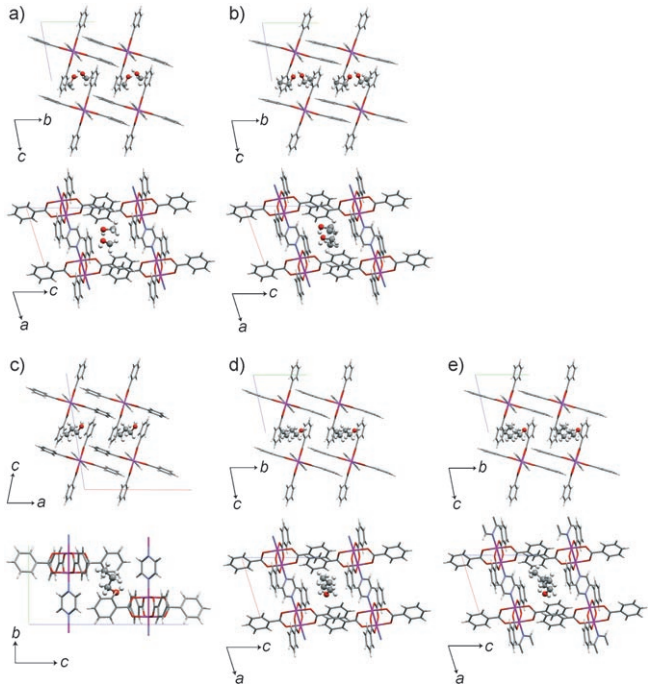

Figure 2. Packing views of the alcohol-inclusion crystals of **1** at 90 K: a) methanol, b) ethanol, c) 1-propanol, d) 1-butanol, and e) 1-pentanol. The projections along the *a* axis (top) and the *b* axis (bottom) are shown in a), b), d), and e). The projections along the *b* axis (top) and the *a* axis (bottom) are shown in c). One of the molecules with centrosymmetric disorder is depicted in the packing. Color code: Rh = magenta, C = gray, H = white, N = blue, O = red.

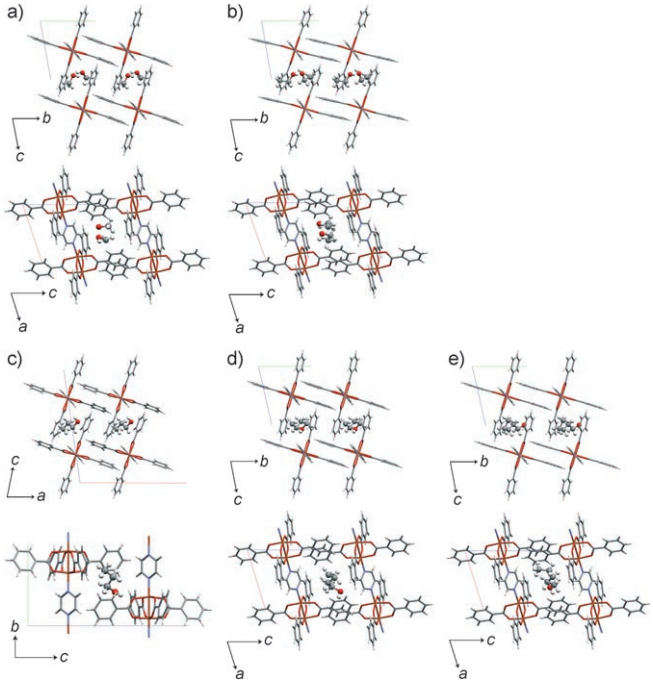

Figure 3. Packing views of the alcohol-inclusion crystals of **2** at 90 K: a) methanol, b) ethanol,[9] c) 1-propanol, d) 1-butanol, and e) 1-pentanol. The projections along the *a* axis (top) and the *b* axis (bottom) are shown in a), b), d), and e). The projections along the *b* axis (top) and the *a* axis (bottom) are shown in c). One of the molecules with centrosymmetric disorder is depicted in the packing. Color code: Cu = orange, C = gray, H = white, N = blue, O = red.

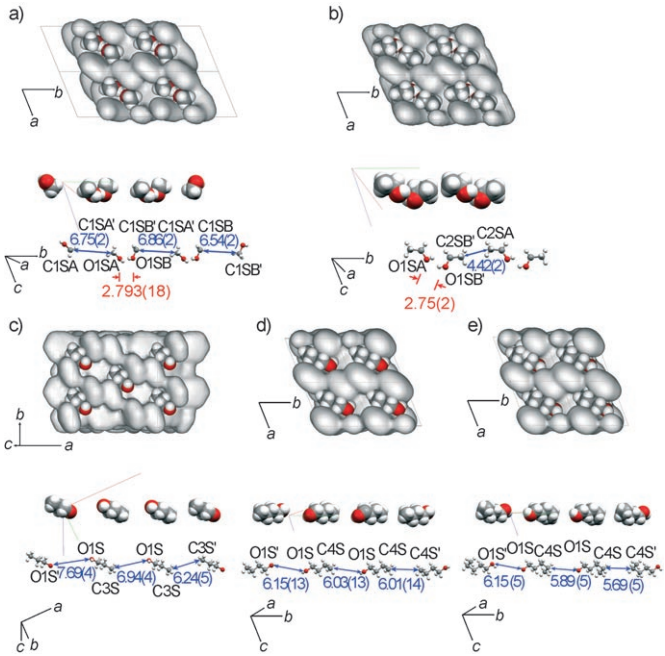

Figure 4. Surface views of the alcohol-inclusion crystals of **1** at 90 K: alcohol aggregate structure (top) and magnified guests (bottom) for a) methanol, b) ethanol, c) 1-propanol, d) 1-butanol, and e) 1-pentanol. One of the molecules with centrosymmetric disorder is depicted with the atomic numbering scheme of the unique atoms. The independent guest–guest distances between disordered molecules are shown.

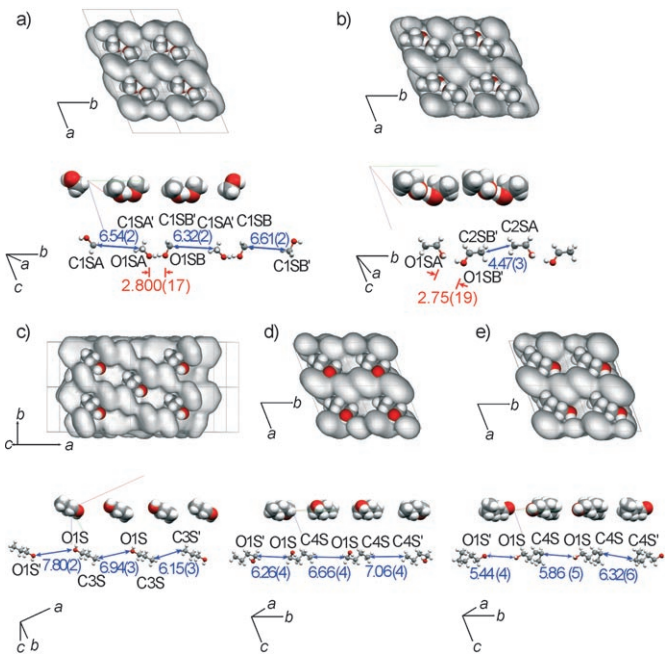

Figure 5. Surface views of the alcohol-inclusion crystals of **2** at 90 K: alcohol aggregate structure (top) and magnified guests (bottom) for a) methanol, b) ethanol,[9] c) 1-propanol, d) 1-butanol, and e) 1-pentanol. One of the molecules with centrosymmetric disorder is depicted with the atomic numbering scheme of the unique atoms. The independent guest–guest distances between disordered molecules are shown.

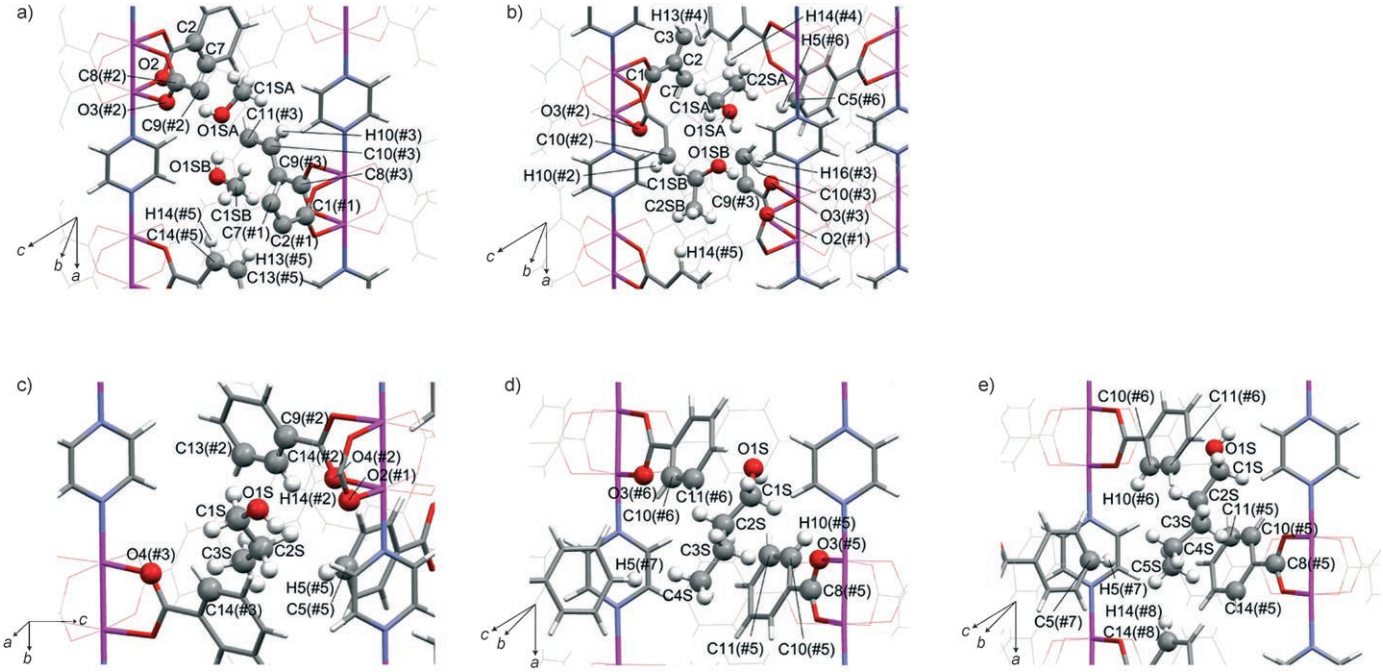

Figure 6. Short contacts between guest molecule and host lattice with the atomic numbering scheme of the unique atoms in **1**: a) methanol, b) ethanol, c) 1-propanol, d) 1-butanol, and e) 1-pentanol. One of the molecules with centrosymmetric disorder is shown within the host cavities.

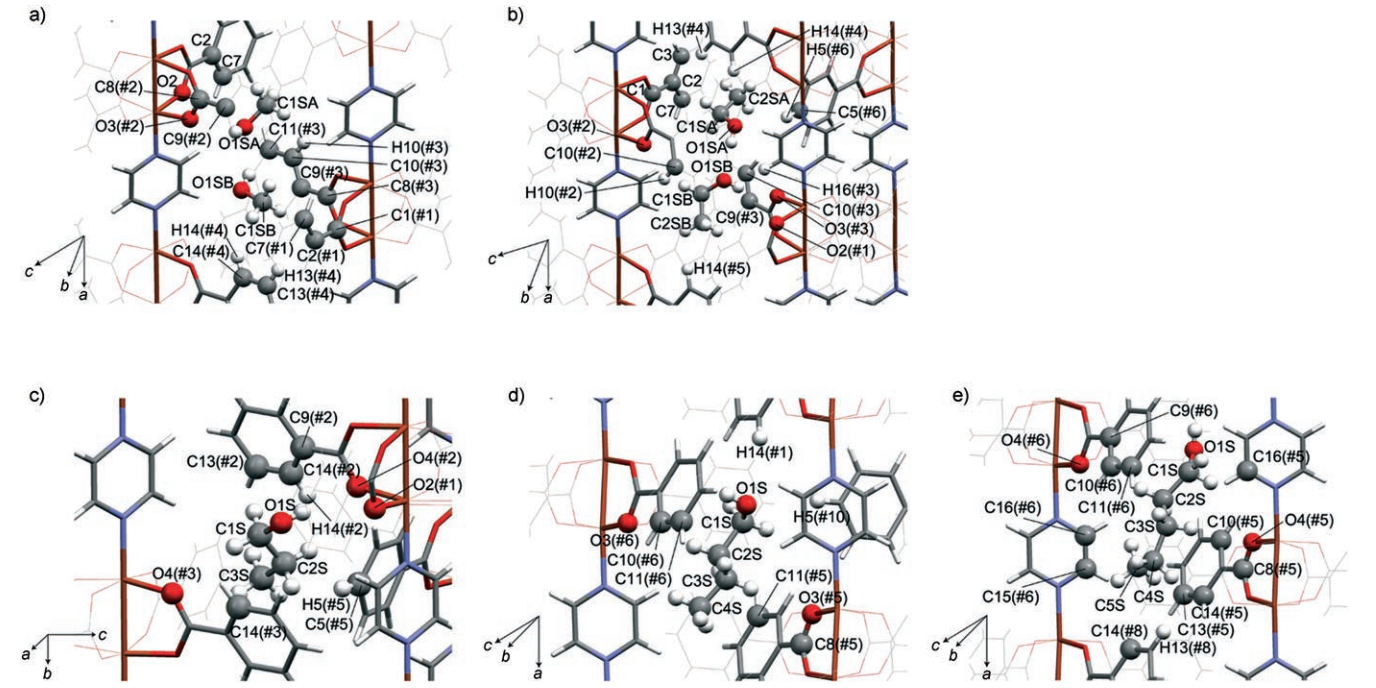

Figure 7. Short contacts between guest molecule and host lattice with the atomic numbering scheme of the unique atoms in **2**: a) methanol, b) ethanol,[9] c) 1-propanol, d) 1-butanol, and e) 1-pentanol. One of the molecules with centrosymmetric disorder is shown within the host cavities.

phobic host wall through alkyl (methyl/methylene)···π interactions (C···C distances were 3.07–3.60 Å for 1-propanol, 3.26–3.28 Å for 1-butanol, and 3.26–3.41 Å for 1-pentanol in both **1** and **2**).

Difference in Aggregate Structures

A clear boundary for guest arrangement, dependent on the alcohol-chain length, was observed between ethanol and 1-propanol. Methanol and ethanol molecules form hydrogen-

Table 3. Host–guest and guest–guest short contacts: pertinent interatomic distances [Å] for methanol- and ethanol-inclusion crystals of **1** and **2**.[a]

1·2CH_3OH		**1**·2C_2H_5OH	
Guest–guest contacts:			
Guest A···B#1			
O1S···O1S#1	2.793(18)	O1S···O1S#1	2.75(2)
O1S···H1S#1	1.957(13)	O1S···H1S#1	3.100(15)
H1S···O1S#1	3.001(11)	H1S···O1S#1	2.113(15)
Host–guest contacts:			
Guest A			
C1S···C2	3.864(15)	C1S···C2	3.512(17)
C1S···C7	3.814(14)	H1S3···C1	2.889(6)
C1S···C8#2	3.665(14)	C2S···C5#6	3.293(16)
C1S···C9#2	3.593(13)	C2S···H5#6	3.142(15)
C1S···O3#2	3.659(16)	C2S···C2	3.543(16)
O1S···O3#2	2.950(8)	C2S···C7	3.575(19)
C1S···C10#3	3.533(17)	C2S···C3	3.688(14)
C1S···C11#3	3.745(18)	C2S···H13#4	3.203(16)
C1S···H10#3	3.068(14)	C2S···H14#4	3.336(17)
O1S···O2	3.293(8)		
Guest B#1			
C1S···C8#3	3.598(14)	O1S···O3#3	2.968(9)
C1S···C9#3	3.599(13)	O1S···O2#1	3.569(10)
C1S···C14#5	3.82(2)	O1S···H16#3	2.637(13)
C1S···C13#5	3.77(2)	H1S2···C9#3	2.875(5)
C1S···C1#1	3.608(13)	H1S2···C10#3	2.950(6)
C1S···C2#1	3.548(13)	C2S···H14#5	3.07(3)
C1S···C7#1	3.641(13)	C1S···C10#2	3.339(16)
C1S···H13#5	3.103(18)	C1S···H10#2	3.024(13)
C1S···H14#5	3.18(2)	H1S3···C10#2	2.639(6)
		H1S3···H10#2	2.2132(2)
		H1S3···O3#2	2.808(3)

2·2CH_3OH		**2**·2C_2H_5OH[9]	
Guest–guest contacts:			
Guest A···B#1			
O1S···O1S#1	2.800(17)	O1S···O1S#1	2.75(1)
O1S···H1S#1	2.124(11)	O1S···H1S#1	3.05(1)
H1S···O1S#1	2.630(12)	H1S···O1S#1	1.92(1)
Host–guest contacts:			
Guest A			
C1S···C2	3.813(15)	C1S···C2	3.55(1)
C1S···C7	3.746(15)	H1S3···C1	3.07(5)
O1S···O2	3.231(8)	C2S···C5#6	3.34(1)
C1S···C8#2	3.730(14)	C2S···H5#6	3.15(1)
C1S···C9#2	3.657(14)	C2S···C2	3.53(1)
O1S···O3#2	3.017(8)	C2S···C7	3.58(1)
C1S···C10#3	3.488(18)	C2S···C3	3.63(1)
C1S···C11#3	3.729(19)	C2S···H13#4	3.18(1)
C1S···H10#3	2.973(15)	C2S···H14#4	3.35(1)
Guest B#1			
C1S···C8#3	3.606(13)	O1S···O3#3	3.031(8)
C1S···C9#3	3.583(13)	O1S···O2#1	3.549(9)
C1S···C13#4	3.80(2)	O1S···H16#3	2.62(1)
C1S···C14#4	3.85(2)	H1S2···C9#3	2.914(4)
C1S···C1#1	3.652(13)	H1S2···C10#3	2.980(6)
C1S···C2#1	3.549(13)	C2S···H14#5	3.22(3)
C1S···C7#1	3.645(13)	C1S···C10#2	3.34(1)
C1S···H13#4	3.122(19)	C1S···H10#2	3.00(1)
C1S···H14#4	3.22(2)	H1S3···C10#2	2.640(6)
		H1S3···H10#2	2.1815(2)
		H1S3···O3#2	2.891(3)

[a] Symmetry codes: #1 = 1−*x*, 1−*y*, 2−*z*, #2 = 2−*x*, 1−*y*, 1−*z*, #3 = −1+*x*, *y*, 1+*z*, #4 = *x*, *y*, 1+*z*, #5 = 1−*x*, 1−*y*, 1−*z*, #6 = 1−*x*, 2−*y*, 2−*z*.

Table 4. Host–guest and guest–guest short contacts: pertinent interatomic distances [Å] for 1-propanol-, 1-butanol-, and 1-pentanol-inclusion crystals of **1** and **2**.[a]

1·0.47*n*-C_3H_7OH		**2**·0.59*n*-C_3H_7OH	
Guest–guest contacts:			
C3S···C3S#4	6.24(5)	C3S···C3S#4	6.24(5)
Host–guest contacts:			
O1S···O2#1	3.41(3)	O1S···O2#1	3.331(17)
O1S···O4#2	3.19(3)	O1S···O4#2	3.327(19)
C1S···C14#2	3.15(5)	C1S···C14#2	3.20(3)
C1S···C14#3	3.07(5)	C1S···C14#3	3.20(3)
H1S1···C9#2	2.733(9)	H1S1···C9#2	2.811(8)
H1S1···C13#2	2.734(8)	H1S1···C13#2	2.792(8)
H1S1···C14#2	2.419(9)	H1S1···C14#2	2.442(9)
H1S2···O4#3	2.627(5)	H1S2···O4#3	2.635(4)
C2S···C14#2	3.26(3)	C2S···C14#2	3.37(2)
C2S···H14#2	2.84(3)	C2S···H14#2	2.91(2)
C2S···H5#4	2.79(4)	C2S···H5#4	2.68(2)
C3S···C5#4	3.60(4)	C3S···C5#4	3.49(2)
1·0.7*n*-C_4H_9OH		**2**·*n*-C_4H_9OH	
Guest–guest contacts:			
C4S···C4S#7	6.01(14)	C4S···C4S#7	6.01(14)
Host–guest contacts:			
C1S···C10#5	3.28(10)	O1S···H5#10	2.687(16)
H1S2···C10#5	2.652(18)	O1S···H14#1	2.60(2)
H1S2···H10#5	2.2044(17)	O1S···C14#6	3.239(14)
C2S···C10#5	3.28(9)	H2S1···C11#5	2.787(7)
H2S1···C10#5	2.635(17)	H2S2···C10#6	2.883(6)
H2S1···C11#5	2.70(2)	H2S2···O3#6	2.626(4)
H2S2···O3#6	2.609(8)	H3S1···C8#5	2.842(6)
H3S1···C8#5	2.810(14)	H3S1···C9#5	2.885(7)
H3S1···O3#5	2.711(11)	H3S1···C10#5	2.829(6)
H3S2···C10#6	2.803(16)	H3S1···O3#5	2.487(4)
H3S2···C11#6	2.74(2)	H3S2···C10#6	2.905(6)
C4S···H5#7	2.61(9)	H3S2···C11#6	2.830(7)
1·0.88*n*-$C_5H_{11}OH$		**2**·0.88*n*-$C_5H_{11}OH$	
Guest–guest contacts:			
C4S···C4S#7	5.69(5)	C4S···C4S#7	5.69(5)
Host–guest contacts:			
C2S···C10#5	3.36(6)	H1S2···C16#5	2.862(15)
H2S1···C10#5	2.588(13)	C2S···C10#6	3.32(5)
H2S1···C11#5	2.797(13)	H2S1···C10#5	2.788(15)
H2S2···C10#6	2.887(12)	H2S2···C9#6	2.790(16)
H3S1···C11#6	2.772(15)	H2S2···C10#6	2.63(15)
H3S2···C8#5	2.797(11)	H2S2···O4#6	2.671(9)
H4S1···C5#7	2.865(18)	H3S1···C10#6	2.750(15)
H4S1···H10#6	2.3437(16)	H3S1···C11#6	2.65(2)
C5S···C14#5	3.28(3)	H3S2···C8#5	2.897(14)
C5S···C14#8	3.34(5)	H3S2···O4#5	2.615(10)
C5S···C15#9	3.27(4)	H4S2···H13#8	2.3230(17)
C5S···H5#7	2.69(4)	C5S···C13#5	3.36(3)
C5S···H14#8	2.45(5)	C5S···C14#5	3.24(3)
		C5S···C14#8	3.41(5)
		C5S···C15#9	3.26(3)
		C5S···C16#6	3.35(3)

[a] Symmetry codes: #1 = 1−*x*, 1−*y*, 1−*z*, #2 = *x*, 1−*y*, 0.5+*z*, #3 = 1−*x*, *y*, 0.5−*z*, #4 = 0.5−*x*, 1.5−*y*, 1−*z*, #5 = 2−*x*, 1−*y*, 1−*z*, #6 = −1+*x*, *y*, 1+*z*, #7 = 1−*x*, −*y*, 2−*z*, #8 = *x*, *y*, 1+*z*, #9 = 2−*x*, 1−*y*, 2−*z*, #10 = *x*, −1+*y*, *z*.

bonded dimers, which also form OH···O hydrogen bonds to the carbonyl O moiety of the host skeleton. In contrast, 1-propanol, 1-butanol, and 1-pentanol molecules are adsorbed in isolated monomeric form without hydrogen-bonding interactions between host and guest. In these cases, the guests

must gain stability through positive interactions between the hydrophobic alkyl moieties and the channel wall. These efficient hydrophobic interactions can overcome the instability in the contact between the hydrophobic host walls and the hydrophilic terminal OH moieties. In the case of 1-propanol inclusion, the alcohol has a relatively short alkyl chain, and positive hydrophobic interactions between host and guest are not significant. The lack of efficient guest stabilization in 1-propanol-inclusion crystals would result in the lowest amount of adsorbed alcohol, as shown in the adsorption measurements (Figure 8). This phenomenon is also caused by the absence of phase transitions, which is only observed in the inclusion crystals of 1-propanol. Thus, the method of stabilizing alcohol molecules in the channels affects the amount of included guest.

Properties of Alcohol-Vapor Adsorption

The vapor-sorption isotherms of **1** and **2** at 293 K are shown in Figure 8. At the saturated vapor pressure, the amounts of adsorbed molecules reached 2.20 (MeOH), 1.75 (EtOH), 0.48 (1-PrOH), and 0.63 mol per Rh_2 unit (1-BuOH) for **1** and 2.48 (MeOH), 2.10 (EtOH),[9] 0.47 (1-PrOH) and 0.74 mol per Cu_2 unit (1-BuOH) for **2**. The amounts of alcohol adsorbed are comparable to those observed in the single-crystal X-ray analysis. Surprisingly, effective adsorption on single-crystal adsorbents **1** and **2** was confirmed by the presence of adsorption for 1-propanol and 1-butanol under diluted guest atmosphere, in spite of the sparseness of the guest molecules in the gas phase as the vapor pressure was decreased ($P_0 = 97.30$ mmHg for methanol, 44.06 mmHg for ethanol, 14.56 mmHg for 1-propanol, 4.42 mmHg for 1-butanol, and 1.43 mmHg for 1-pentanol at 293 K). Although the analysis of 1-pentanol was difficult because of its extremely low vapor pressure, its adsorption amount is expected to be almost equivalent to that observed for 1-butanol from the results of X-ray diffraction analysis. The channel spaces of **1** and **2** are capable of accommodating up to two ethanol molecules.[9] The small adsorption quantity of 1-propanol and 1-butanol is due to the increase in the guest volume for the occupation of the channel as the alkyl chain becomes longer. Although 1-propanol is midsized and has a higher vapor pressure than 1-butanol, the smallest number of adsorbed molecules was found for 1-propanol adsorption. This difference reflects the relatively low stabilization of the 1-propanol molecules in the channel space, as discussed in the structural description (see above).

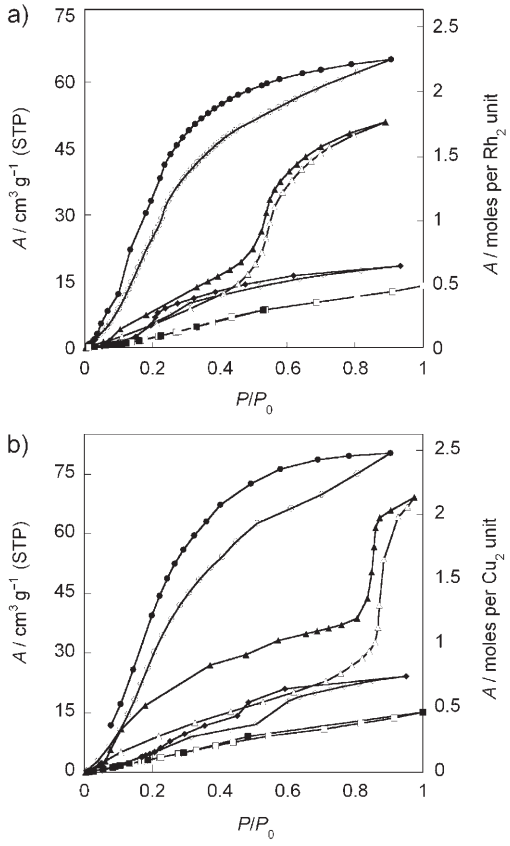

Figure 8. Sorption isotherms for single crystals of a) **1** and b) **2** at 293 K: methanol (circles), ethanol (triangles), 1-butanol (diamonds), 1-propanol (squares); adsorption (open symbols), desorption (solid symbols). The volume of adsorbed alcohol is represented by a unit converted into standard conditions (STP: 0 °C, 0.1 MPa). A = amount of adsorbed alcohol.

In the case of ethanol vapor, an ideal, almost-vertical jump in adsorption was observed in both hosts between 15 and 40 $cm^3 g^{-1}$ (STP) for **1** and between 20 and 60 $cm^3 g^{-1}$ (STP) for **2**. We previously reported that the jump in adsorption for **2** is caused by the bulk phase transition accompanied by the crystal-phase transition from a monoclinic to a triclinic system.[9] This phenomenon was proposed as a "mass (amount of adsorbed guest)-induced phase transition", which is essentially different from the usual temperature- or pressure-induced transition, as the current transition is triggered by gas-adsorption phenomena, which changes the chemical composition of the inclusion crystal.[9] This bulk phase transition is caused by the adsorption of around one molecule per M_2 unit, which is similar to the critical quantity observed in CO_2-adsorption processes.[6,8b,9] Although the adsorption behavior of **1** and **2** are essentially the same for the respective alcohols, the critical pressures are considerably different, that is, 0.48 mmHg for **1** and 0.85 mmHg for **2** (EtOH),[9] and 0.20 mmHg for **1** and 0.50 mmHg for **2** (1-BuOH). The jumps in adsorption observed in **1** indicate that the phase transition occurs at a lower relative pressure with slightly lower adsorption amounts than in **2**.

In methanol adsorption, the beginning of the bulk phase transition, the jump in adsorption, is difficult to distinguish in the isotherms, which indicates a deviation from the ideal system observed in ethanol. With respect to the cavity, the methanol monomer is not large enough for the potential critical state required to cause the phase transition. However, the hydrogen-bonded methanol dimer would pass the critical state. The hydrogen-bonding interaction for methanol is stronger than for ethanol. However, because of its small size, the methanol dimer is less stable than the ethanol dimer in the cavity that can incorporate the latter in a β-

phase crystal. In contrast, inclusion of the methanol monomer has little influence on the stress on the cavity structure of the α-phase crystal without the phase transition; the monomer is thus sufficiently stabilized by the host wall. Therefore, these two possible states are expected to be generated competitively during methanol-vapor inclusion, and would result in an unclear phase transition with a more-gradual rise in adsorption. The fluctuation of the multiple-guest states during the transition process of methanol may apparently behave as a higher-order rather than a simple first-order transition.

In the case of 1-butanol, the jump in adsorption was observed in the isotherms between 5 and 10 $cm^3 g^{-1}$ (STP) for **1** and between 12 and 19 $cm^3 g^{-1}$ (STP) for **2**; the jump in adsorption thus begins when rather low amounts are adsorbed ($\approx$0.3 and $\approx$0.5 mol per M_2 unit for **1** and **2**, respectively). Because the molecular volume of 1-butanol is larger than that of ethanol, the potential critical state for the phase transition can be passed on the microscopic scale even by the inclusion of one molecule in each channel unit. Therefore, on the macroscopic scale, 1-butanol molecules can cause a crystal-phase transition even with small amounts of adsorbed guests by generating the β-phase domain involving the surrounding empty cavities. However, the imperfect guest distribution in the domains passing the critical point in the crystal would make the bulk-phase-transition point ambiguous in adsorption measurements. The phase transition of 1-pentanol inclusion crystals (triclinic; see above) is also expected to occur with a small quantity of adsorbed guests due to its large molecular volume.

In 1-propanol, a continuous increase in amount of adsorption was observed without a distinct jump, which is in agreement with the absence of phase transitions in the 1-propanol inclusion, as was confirmed by structural analysis. Because the 1-propanol molecule cannot effectively gain stabilization by the host wall in the cavity as discussed above, the amounts adsorbed do not increase. The small amount of 1-propanol adsorption is insufficient to generate domains that result in a bulk phase transition.

An adsorption hysteresis was clearly found only in the methanol and ethanol vapor-sorption curves; this indicates a difference between the adsorption and desorption processes. Given the ability of methanol and ethanol to associate in the host crystals by hydrogen bonding, the hysteresis seems to correlate with the association/dissociation of the hydrogen-bonded dimer, as suggested in the previous study for ethanol inclusion in **2**.[9] At high temperature, the included guest can be thermally excited from the stable dimer to an isolated monomer through hydrogen-bond dissociation. The mixing and exchange of dimer and monomer states would cause a large hysteresis loop in the adsorption isotherm for methanol, which was perhaps further influenced by the fluctuation of the host structures through the changing of the guest states. Hysteresis in 1-propanol and 1-butanol was negligible owing to a simple mechanism of adsorption and diffusion without the generation of a hydrogen-bonded dimer within the channel.

On a microscopic scale, each channel unit includes an integral number of guest molecules (0, 1, 2), although bulk measurements such as adsorption isotherms give the ensemble average properties macroscopically. Consequently, the microscopic state should be explained by stepwise inclusion into the individual cavities (Figure 9), which can be called

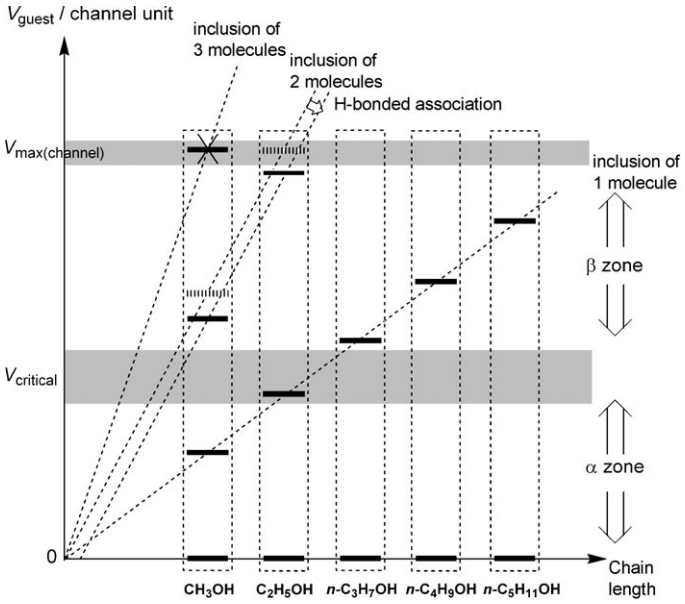

Figure 9. Relationship between chain length and guest volume for guests occupying a channel unit. The gray zones display the practical volume range on the macroscopic scale corresponding to the boundary between the phases changed by the bulk phase transformation.

the "step-loading effect." The correlation between guest chain length and guest volume for occupation of the cavity unit is shown schematically in Figure 9. There is a significant correlation between guest volume and critical volume ($V_{critical}$), which qualifies to cause the bulk phase transition. As the chain length of the guest alcohol increases, the guest volume increases linearly. Thus, the limitation of the practical inner space of the channel restricts the number and structure of the included alcohol. Because the adsorption of one ethanol molecule per channel unit gives a guest volume of around $V_{critical}$, ethanol inclusion can be regarded as the ideal system for **1** and **2**. The integral number of adsorbed molecules per channel unit strongly indicates that the state of adsorption depends not on the total potential volume of the channel but on the arrangement of the included guests according to the structure and symmetry of the channel units. The flexible channel space is transformed to stabilize the cocrystallized state of the guest inclusion. This structural adjustment compensates for the instability caused by the excess of or deficiency in inner-space volume in including guest molecules under various loaded states.

Alcohol/Water Separation

Pervaporation measurements were performed on a standard pervaporation apparatus[19] at room temperature. As crystals

1 and **2** have hydrophobic channels, specific selectivity in the separation of alcohol from a mixture with water is expected from the application of these crystals as separation membranes. We succeeded in preparing a membrane of microcrystals **2** with a concentration of 3 wt% supported by PDMS with the appropriate strength required (Figure 10). The layer thickness, diameter, and effective surface area of the membrane were about 300 μm, 3.5 cm, and 7.0 cm^2, respectively. The mass of alcohol in the water/alcohol feed mixture was 5 wt%. The flux (Q) and separation factor (α) were estimated by Equations (1) and (2), respectively:

$$Q = \frac{w}{St} \quad (1)$$

$$\alpha = \frac{y_A/y_B}{x_A/x_B} \quad (2)$$

in which w is the weight of permeate, S is the effective membrane area, t is the permeation time, x_A and x_B are the volume fractions of alcohol and H_2O, respectively, in the feed, and y_A and y_B are the volume fractions of alcohol and H_2O, respectively, in the permeate.

The separation factors obtained are summarized in Table 5. As opposed to the blank membrane, which gave the concentration of alcohol in the permeate with an α value of about 2.0, the PDMS membrane with microcrystals of **2** produced an α value more than three times greater. Furthermore, the flux values were slightly higher than those of the blank membrane. These results provide convincing evidence that the adsorbed alcohol molecule in **2** diffuses through the crystal and is desorbed on the permeate side without being blocked. The increase in α and Q were achieved even with a low concentration of crystals (3 wt%). Thus, a membrane with high substrate content and is self-supporting is expected to perform extremely well in separation.

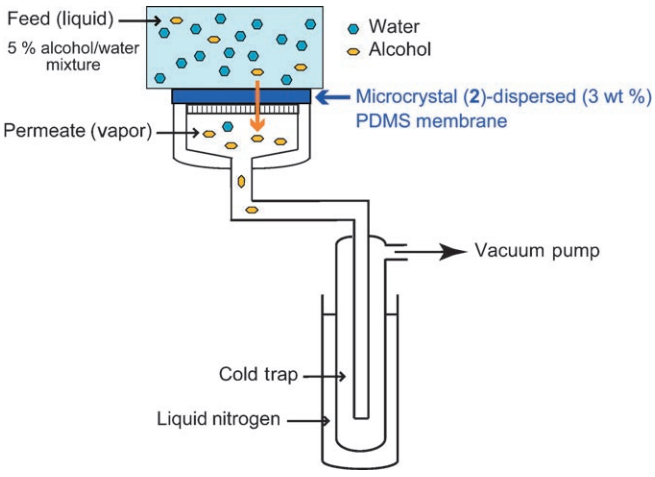

Figure 10. Alcohol separation by pervaporation.

Table 5. Pervaporation results[a] for methanol and ethanol separation with the microcrystal-dispersed PDMS membrane of **2**.[b]

Membrane	α		Q [$kg\,m^{-2}\,h^{-1}$]	
	MeOH	EtOH	MeOH	EtOH
PDMS only (blank)	2.0	2.3	2.4×10^{-2}	2.3×10^{-2}
PDMS with **2**	6.5	6.2	3.3×10^{-2}	4.7×10^{-2}

[a] Conditions: Thickness of membrane about 300 μm, temperature 298 K, feed concentration 5 wt% alcohol in water/alcohol mixture. [b] Concentration of microcrystals of **2**: 3 wt%.

Conclusions

The single-crystal adsorbents $[M^{II}_2(bza)_4(pyz)]_n$ (M = Rh (**1**), Cu (**2**)) absorb the alcohols methanol, ethanol, 1-propanol, 1-butanol, and 1-pentanol. In spite of the possible multiconfiguration and multistabilization of the guest, the cavities in **1** and **2** generate a uniform array of guests according to the guest species (the hydrogen-bonded dimer of methanol and ethanol, and the monomer of 1-propanol, 1-butanol, and 1-pentanol) by cocrystallization. In the cavities, hydrophilic and/or hydrophobic interactions between host and guest stabilize the adsorbed alcohols. However, the difference in the degree of guest stabilization within the cavity clearly influences the amount adsorbed, the occurrence of the macroscopic phase transition, and the hysteresis behavior in the adsorption measurements. The adsorption behavior, the aggregate structure of the incorporated guest, the change in partial structure, and the bulk phase transition are closely related to one another through molecular-level phenomena and long-range ordering. Pervaporation with crystal **2** indicated the selective adsorption and diffusion of the alcohol molecules in the channel. The single-crystal adsorbents of **1** and **2** would be useful for recognizing guest molecules to produce selective aggregate structures and to separate desired molecules directly from the mixture.

It should be emphasized that the present single-crystal host is not very "solid"; rather, it is flexible, with some potential degree of freedom even in its crystalline state. Therefore, through weak physical-adsorption interactions, a change in solid structure (local structure, pore structure, guest aggregation, guest conformation, crystal structure) can occur easily and stabilize the state of various guests. Here, the relationship between the incorporated guest and the walls of the subnanospaces can be compared to the atomic contact of a point (atom) to a point (atom). As the dynamic gas-sorption phenomena and smooth guest transfer correlate with the flexibility of the host crystal and the arrangement of the included guest, novel dynamic selectivity for gas concentration, storage/release, separation, and so on is to be expected. The homogeneity, anisotropy, integrity, transparency, and so on of crystal adsorbents will contribute to the advancement of new techniques for future technologies.

Experimental Section

Single-Crystal X-ray Diffraction Experiment

Single-crystal adsorbents **1** and **2** were synthesized according to the method in the literature.[5,6] Single-crystal X-ray analysis was performed

on a Bruker SMART APEX CCD area diffractometer (graphite-monochromated $Mo_{K\alpha}$ radiation ($\lambda = 0.71073$ Å)) with a nitrogen-flow temperature controller. Alcohol-inclusion crystals were prepared by exposure to the respective alcohol vapor at room temperature in a glass capillary by a method similar to that reported in reference [9]. Data collection was performed at 90 K for all guest-inclusion crystals. Empirical absorption corrections were applied by using the SADABS program. The structures were solved by direct methods (SHELXS-97) and refined by full-matrix least-squares calculations on F^2 (SHELXL-97) with the SHELX-TL program package. Non-hydrogen atoms were refined anisotropically; hydrogen atoms were fixed at calculated positions and refined by using a riding model. Crystallographic data of the structure determination collected under different conditions are summarized in Tables 1 and 2. CCDC-629136–629144 (**1**·2CH_3OH, **1**·2C_2H_5OH, **1**·0.47*n*-C_3H_7OH, **1**·0.7*n*-C_4H_9OH, **1**·0.88*n*-$C_5H_{11}OH$, **2**·2CH_3OH, **2**·0.59*n*-C_3H_7OH, **2**·*n*-C_4H_9OH, and **2**·0.88*n*-$C_5H_{11}OH$, respectively) contain the supplementary crystallographic data for this paper. These data can be obtained free of charge from The Cambridge Crystallographic Data Centre at http://www.ccdc.cam.ac.uk/data request/cif.

Physical Measurements

The vapor-adsorption isotherms for all the alcohols except 1-pentanol were recorded on a Quantachrome Autosorb-1-VP at a relative pressure (P/P_0, P_0 = saturated vapor pressure) ranging from 0.003 to 0.999 (with P_0 = 97.30, 44.06, 14.56, 4.412 mmHg for methanol, ethanol, 1-propanol, and 1-butanol, respectively, at 293 K).

The PDMS used as the matrix for the microcrystals of **2** (3 wt %) was purchased from Shinetsu Chemical and used without further purification. Two-component PDMS polymers with the microcrystals of **2** were mixed in a poly(tetrafluoroethylene) (PTFE) beaker to give a homogeneous suspension. The suspension was placed onto a PTFE plate and heated at 100 °C for 24 h until the membrane was formed. The effective membrane area was 7.0 cm^2; the thickness was about 300 μm. An aqueous alcohol solution (5 wt %) was used as a feed. The permeation was trapped by a cold trap with liquid nitrogen as a coolant. The compositions of the feed and the permeation were determined by gas chromatography.

Acknowledgements

This work was financially supported by the Ministry of Education, Culture, Sports, Science, and Technology, Japan (No. 18750051 and 18033043), a 2006 Strategic Research Project grant from Yokohama City University (No. K18031 and K18032), and the Asahi Glass Foundation.

[1] a) O. M. Yaghi, M. O'Keeffe, N. W. Ockwig, H. K. Chae, M. Eddaoudi, J. Kim, *Nature* **2003**, *423*, 705–713; b) S. Kitagawa, R. Kitaura, S. Noro, *Angew. Chem.* **2004**, *116*, 2388–2430; *Angew. Chem. Int. Ed.* **2004**, *43*, 2334–2375; c) G. Férey, C. Mellot-Draznieks, C. Serre, F. Millange, *Acc. Chem. Res.* **2005**, *38*, 217–225; d) D. Bradshaw, J. B. Claridge, E. J. Cussen, T. J. Prior, M. J. Rosseinsky, *Acc. Chem. Res.* **2005**, *38*, 273–282; e) S. Kitagawa, K. Uemura, *Chem. Soc. Rev.* **2005**, *34*, 109–119; f) A. J. Fletcher, K. M. Thomas, M. J. Rosseinsky, *J. Solid State Chem.* **2005**, *178*, 2491–2510; g) W. Mori, S. Takamizawa in *Organometallic Conjugation* (Eds.: A. Nakamura, N. Ueyama, K. Yamaguchi), Kodansha Springer, Tokyo, **2002**, chap. 6, pp. 179–213.

[2] a) M. Yoshizawa, K. Kumazawa, M. Fujita, *J. Am. Chem. Soc.* **2005**, *127*, 13456–13457; b) M. Kawano, Y. Kobayashi, T. Ozeki, M. Fujita, *J. Am. Chem. Soc.* **2006**, *128*, 6558–6559; c) M. Yoshizawa, M. Tamura, M. Fujita, *Science* **2006**, *312*, 251–254; d) T. Uemura, S. Horike, S. Kitagawa, *Chem. Asian J.* **2006**, *1–2*, 36–44.

[3] For examples: a) K. Uemura, S. Kitagawa, M. Kondo, K. Fukui, R. Kitaura, H.-C. Chang, T. Mizutani, *Chem. Eur. J.* **2002**, *8*, 3586–3600; b) C. Serre, F. Millange, C. Thouvenot, M. Nogues, G. Marsolier, D. Louër, G. Férey, *J. Am. Chem. Soc.* **2002**, *124*, 13519–13526; c) R. Kitaura, K. Seki, G. Akiyama, S. Kitagawa, *Angew. Chem.* **2003**, *115*, 444–447; *Angew. Chem. Int. Ed.* **2003**, *42*, 428–431; d) T. Loiseau, C. Serre, C. Huguenard, G. Fink, F. Taulelle, M. Henry, T. Bataille, G. Férey, *Chem. Eur. J.* **2004**, *10*, 1373–1382; e) K. Yamada, S. Yagishita, H. Tanaka, K. Tohyama, K. Adachi, S. Kaizaki, H. Kumagai, K. Inoue, R. Kitaura, H.-C. Chang, S. Kitagawa, S. Kawata, *Chem. Eur. J.* **2004**, *10*, 2647–2660; f) K. Yamada, H. Tanaka, S. Yagishita, K. Adachi, T. Uemura, S. Kitagawa, S. Kawata, *Inorg. Chem.* **2006**, *45*, 4322–4324.

[4] a) D. Braga, F. Grepioni, *Chem. Soc. Rev.* **2000**, *29*, 229–238; b) E. Y. Lee, M. P. Suh, *Angew. Chem.* **2004**, *116*, 2858–2861; *Angew. Chem. Int. Ed.* **2004**, *43*, 2798–2801; c) K. Takaoka, M. Kawano, M. Tominaga, M. Fujita, *Angew. Chem.* **2005**, *117*, 2189–2192; *Angew. Chem. Int. Ed.* **2005**, *44*, 2151–2154; d) G. J. Halder, C. J. Kepert, *J. Am. Chem. Soc.* **2005**, *127*, 7891–7900; e) T. K. Maji, G. Mostafa, R. Matsuda, S. Kitagawa, *J. Am. Chem. Soc.* **2005**, *127*, 17152–17153; f) E. C. Spencer, J. A. K. Howard, G. J. McIntyre, J. L. C. Rowsell, O. M. Yaghi, *Chem. Commun.* **2006**, 278–280.

[5] S. Takamizawa, T. Hiroki, E. Nakata, K. Mochizuki, W. Mori, *Chem. Lett.* **2002**, *31*, 1208–1209.

[6] S. Takamizawa, E. Nakata, H. Yokoyama, *Inorg. Chem. Commun.* **2003**, *6*, 763–765.

[7] R. Nukada, W. Mori, S. Takamizawa, M. Mikuriya, M. Handa, H. Naono, *Chem. Lett.* **1999**, *28*, 367–368.

[8] a) S. Takamizawa, E. Nakata, T. Saito, K. Kojima, *CrystEngComm* **2003**, *5*, 411–413; b) S. Takamizawa, E. Nakata, H. Yokoyama, K. Mochizuki, W. Mori, *Angew. Chem.* **2003**, *115*, 4467–4470; *Angew. Chem. Int. Ed.* **2003**, *42*, 4331–4334; c) S. Takamizawa, E. Nakata, T. Saito, *Inorg. Chem. Commun.* **2003**, *6*, 1415–1418; d) S. Takamizawa, E. Nakata, T. Saito, *Angew. Chem.* **2004**, *116*, 1392–1395; *Angew. Chem. Int. Ed.* **2004**, *43*, 1368–1371; e) S. Takamizawa, E. Nakata, T. Saito, *Inorg. Chem. Commun.* **2004**, *7*, 1–3; f) S. Takamizawa, E. Nakata, T. Saito, *Chem. Lett.* **2004**, *33*, 538–539; g) S. Takamizawa, E. Nakata, *CrystEngComm* **2005**, *7*, 476–479; h) S. Takamizawa, E. Nakata, T. Saito, T. Akatsuka, K. Kojima, *CrystEngComm* **2004**, *6*, 197–199; i) S. Takamizawa, E. Nakata, T. Saito, T. Akatsuka, *Inorg. Chem.* **2005**, *44*, 1362–1366; j) S. Takamizawa, E. Nakata, T. Akatsuka, *Angew. Chem.* **2006**, *118*, 2274–2279; *Angew. Chem. Int. Ed.* **2006**, *45*, 2216–2221.

[9] S. Takamizawa, T. Saito, T. Akatsuka, E. Nakata, *Inorg. Chem.* **2005**, *44*, 1421–1424.

[10] a) J. W. Johnson, A. J. Jacobson, W. M. Butler, S. E. Rosenthal, J. F. Brody, J. T. Lewandowski, *J. Am. Chem. Soc.* **1989**, *111*, 381–383; b) M. R. Torgerson, D. G. Nocera, *J. Am. Chem. Soc.* **1996**, *118*, 8739–8740; c) D. V. Soldatov, J. A. Ripmeester, *Chem. Mater.* **2000**, *12*, 1827–1839; d) K. Sada, M. Sugahara, K. Kato, M. Miyata, *J. Am. Chem. Soc.* **2001**, *123*, 4386–4392; e) A. P. Côte, M. J. Ferguson, K. A. Khan, G. D. Enright, A. D. Kulynych, S. A. Dalrymple, G. K. H. Shimizu, *Inorg. Chem.* **2002**, *41*, 287–292; f) H. J. Choi, M. P. Suh, *J. Am. Chem. Soc.* **2004**, *126*, 15844–15851.

[11] a) L. Y. Lu, A. M. Babb, *Chem. Commun.* **2002**, 1340–1341; b) M.-H. Zeng, X.-L. Feng, X.-M. Chen, *Dalton Trans.* **2004**, 2217–2223; c) M.-H. Zeng, X.-L. Feng, W.-X. Zhang, X.-M. Chen, *Dalton Trans.* **2006**, 5294–5303.

[12] a) L. Pan, K. M. Adams, H. E. Hernandez, X. Wang, C. Zheng, Y. Hattori, K. Kaneko, *J. Am. Chem. Soc.* **2003**, *125*, 3062–3067; b) D. N. Dybtsev, H. Chun, S. H. Yoon, D. Kim, K. Kim, *J. Am. Chem. Soc.* **2004**, *126*, 32–33; c) T. K. Maji, K. Uemura, H.-C. Chang, R. Matsuda, S. Kitagawa, *Angew. Chem.* **2004**, *116*, 3331–3334; *Angew. Chem. Int. Ed.* **2004**, *43*, 3269–3272; d) R. Matsuda, R. Kitaura, S. Kitagawa, Y. Kubota, R. V. Belosludov, T. C. Kobayashi, H. Sakamoto, T. Chiba, M. Takata, Y. Kawazoe, Y. Mita, *Nature* **2005**, *436*, 238–241; e) L. Pan, D. H. Olson, L. R. Ciemnolonski, R. Heddy, J. Li, *Angew. Chem.* **2006**, *118*, 632–635; *Angew. Chem. Int. Ed.* **2006**, *45*, 616–619.

[13] J. L. Atwood, L. J. Barbour, A. Jerga, *Angew. Chem.* **2004**, *116*, 3008–3010; *Angew. Chem. Int. Ed.* **2004**, *43*, 2948–2950.

[14] B. Chen, C. Liang, J. Yang, D. S. Contreras, Y. L. Clancy, E. B. Lobkovsky, O. M. Yaghi, S. Dai, *Angew. Chem.* **2006**, *118*, 1418–1421; *Angew. Chem. Int. Ed.* **2006**, *45*, 1390–1393.

[15] Review: L. M. Vane, *J. Chem. Technol. Biotechnol.* **2005**, *80*, 603–629.
[16] Reviews: a) T. Bein, *Chem. Mater.* **1996**, *8*, 1636–1653; b) A. Tavolaro, E. Drioli, *Adv. Mater.* **1999**, *11*, 975–996; c) T. C. Bowen, R. D. Noble, J. L. Falconer, *J. Membr. Sci.* **2004**, *245*, 1–33.
[17] Crystal data for empty host **1** at 93 K: monoclinic, *C*2/*c* (No. 15), $a=17.42(3)$, $b=9.55(1)$, $c=19.70(4)$ Å, $\alpha=90(2)$, $\beta=98.05(6)$, $\gamma=90°$, $V=3244(9)$ Å^3, $Z=4$.[8b]
[18] Crystal data for empty host **2** at 93 K: monoclinic, *C*2/*c* (No. 15), $a=17.631(10)$, $b=9.704(4)$, $c=19.220(10)$ Å, $\alpha=90$, $\beta=98.14(4)$, $\gamma=90°$, $V=3255(2)$ Å^3, $Z=4$.[6]
[19] T. Sano, M. Hasegawa, Y. Kawakami, H. Yanagishita, *J. Membr. Sci.* **1995**, *107*, 193–196.

Received: December 5, 2006
Revised: April 2, 2007
Published online: May 24, 2007

